OTC 23166

Wind Effect Estimation and Navigational Effect in Side by Side Offloading Operation for FLNG and LNG Carrier Ships

Toshifumi Fujiwara, Kazuhiro Yukawa, Hiroshi Sato, Shunji Kato, National Maritime Research Institute, Japan

Abstract

The side by side offloading operation for a Floating LNG facility (FLNG) and a LNG carrier ship (LNG) is expected efficient way of offloading rather than tandem style one, since the ondeck equipment is easily installed using the common facility used in the port terminal. In case of considering the LNG approaching to the FLNG, however, it is needed to pay attention for the weather condition like wind, waves and current. Rapidly change of those weather conditions causes the difficulty of manoeuvring of the LNG, and in worst the LNG may crash to the FLNG. In particular a conventional LNG has large superstructures and the operating speed of the LNG is very slow at the closed navigational area for the FLNG. Wind effect becomes larger than the other operational situation in the ocean. Then the operational capability evaluation of the LNG would be needed to grasp the operational weather limitation. The effect of each element on weather conditions, that is wind etc. giving manoeuvring difficulty to ships as external load, is expected to assess exactly. Wind interaction effect under the operating condition that a FLNG and a LNG are in same closed area, however, is not clearly understood. This paper treats and proposes one estimation method of wind load including interaction effect of a FLNG and a LNG for the operation of side-by-side offloading. The proposed wind load estimation method based on the wind tunnel experiments sufficiently represents the shielding effect of interaction of the LNG behind the FLNG. Operational assessment on ship manoeuvring under strong wind is calculated using the proposed wind load estimation method in the final stage.

1 Introduction

The gross area of the sea on the earth is vast and the percentage which accounts for a whole surface of the earth is about 71%. In considering the securing of resources on Liquid Natural Gas (LNG), the region of the development spreads out from land to the sea recently and sea excavating points of that are expanded from shallow sea area to deep ocean gradually. When getting LNG in the ground under the sea distant from land, it will be necessary to transfer the LNG from the excavating and production facility to a transport ship after producing it at those points.

In such a situation, LNG offloading critical limitation under rough sea is important information for the operation of transferring storage LNG resource from a Floating LNG facility (FLNG) to a LNG carrier ship (LNG as a ship). The side by side offloading operation, see Figure 1 as the image, to supply liquid gas from the FLNG to the LNG is adopted frequently with easier operational reason rather than tandem style operation. In the side by side offloading operation, however, weather condition must be paid attention enough to prevent the collision accident between the FLNG and the LNG.

The authors have focused on the wind shielding effect in side by side offloading situation of operating ships in this paper. In the past presented papers by another authors [1]~[4], general information noted the importance of consideration for the wind shielding effect was pointed out, and in some cases, CFD (Computational Fluid Dynamics) calculations in the ship shielding conditions had conducted[4]. Detail analysis of the effect based on experimental or the wind shielding effect on calculated results, however, have not generally presented in them. Easier estimation method or logic of assessing on ship shielding conditions is expected to get information for operational risk from the viewpoints of practical use.

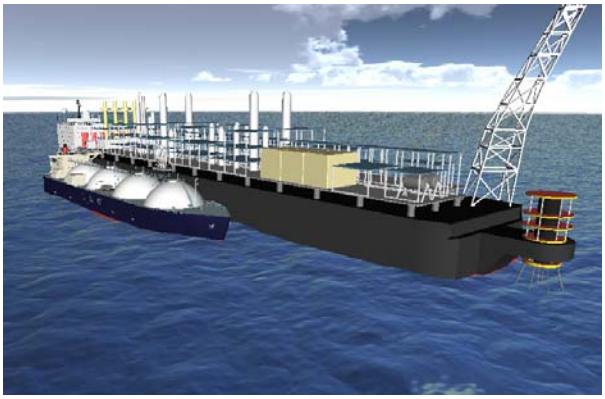

Figure 1. Image sample picture in case of side by side offloading operation of FLNG & LNG.

Then an attempt on wind load estimation method for a LNG with the shielding effect is presented in this paper. Initially the wind tunnel experiments and results for a FLNG and a LNG models in the side by side situation are presented. The experiments were carried out in our research institute in order to grasp aerodynamic specification for those models. Many kinds of each other positions for the FLNG and the LNG were set in the experiments. Secondly using those experimental results, some aerodynamic specific theories are clarified, and it is shown the estimation method for wind load including the shielding effect to be able to use in the ships with side by side situation and approaching. This method is simply based on the geometrical ship position and external form. Finally the shielding effect in the FLNG-LNG carrier ships operation is also presented using the ship manoeuvring simulation in wind in the final paper stage. The calculated result for the LNG drift motion presents the importance of the evaluation of the FLNG shielding effect to estimate operational risk on the side by side situation.

2 Wind tunnel experiments

2.1 Sample ships:

The sample ships on a FLNG and a LNG shown in Table 1 are used in the experiments and calculations in this paper. Here in the table, L_{OA}; the overall length, L_{PP}; the length between perpendiculars, B; the breadth, D; the draught, d; the depth, A_F; the frontal projected area, A_L; the lateral projected area and A_{OD}; the lateral projected area of superstructure etc. on the deck. Moreover, C; the horizontal distance from amidships section to center of lateral projected area, H_C; the height from calm water surface to center of lateral projected area, H_B; the height of top of superstructure (bridge etc.) are included in the table (See Figure 6 for better understanding). Those ships are typical size of the gas loading operation. A moss type one with 4 large spherical tanks on the deck is treated as the LNG sample ship.

Table 1. Principal particulars of the sample ships on fully loaded FLNG and ballasted LNG (1/200 models).

FLNG (Full)

	Unit	Ship	Model
L_{OA}	m	336.0	1.680
L_{PP}	m	328.6	1.643
B	m	50.0	0.250
D	m	31.6	0.158
d	m	12.2	0.061
A_F	m^2	2482	0.062
A_L	m^2	10126	0.253
A_{OD}	m^2	4200	0.105
C	m	-3.4	-0.017
H_C	m	19.7	0.099
H_B	m	46.2	0.231

LNG (Ballast)

	Unit	Ship	Model
L_{OA}	m	289.5	1.448
L_{PP}	m	277.0	1.385
B	m	49.0	0.245
D	m	27.0	0.135
d	m	9.4	0.047
A_F	m^2	1885	0.047
A_L	m^2	8855	0.221
A_{OD}	m^2	4087	0.102
C	m	-3.7	-0.019
H_C	m	15.3	0.077
H_B	m	47.3	0.237

2.2 Coordinate system of wind forces:

The wind shielding effect in side by side offloading situation of operating ships is considered. The LNG is in behind the larger FLNG. Figure 2 defines the cartesian x-y coordinate reference system for the wind forces and moments used in the paper and the interrelationship position of the FLNG and the LNG. The origin for the main object, in this case of LNG, is located the amidship at the intersection of the still water place and on the longitudinal line of ship symmetry. Figure 2 also provides definitions and associated sign conventions for the longitudinal force X_A, the lateral force Y_A and the yaw, heel moments N_A, K_A. The apparent angle of attack of the wind relative to the positive x-axis of the ship is defined as ψ_A. The non-dimensional form of the longitudinal, lateral forces and yaw, heel moments are defined as follows:

$$\begin{aligned} C_X(\psi_A) &= X_A(\psi_A)/(q_A A_F) \\ C_Y(\psi_A) &= Y_A(\psi_A)/(q_A A_L) \\ C_N(\psi_A) &= N_A(\psi_A)/(q_A A_L L_{OA}) \\ C_K(\psi_A) &= K_A(\psi_A)/(q_A A_L H_L) \end{aligned} \tag{1}$$

where,

$$q_A = \frac{1}{2}\rho_A U_A^2 \tag{2}$$

with ρ_A; the indicating air density, U_A; the apparent wind velocity, H_L; the mean height of a ship (equal to A_L / L_{OA}).

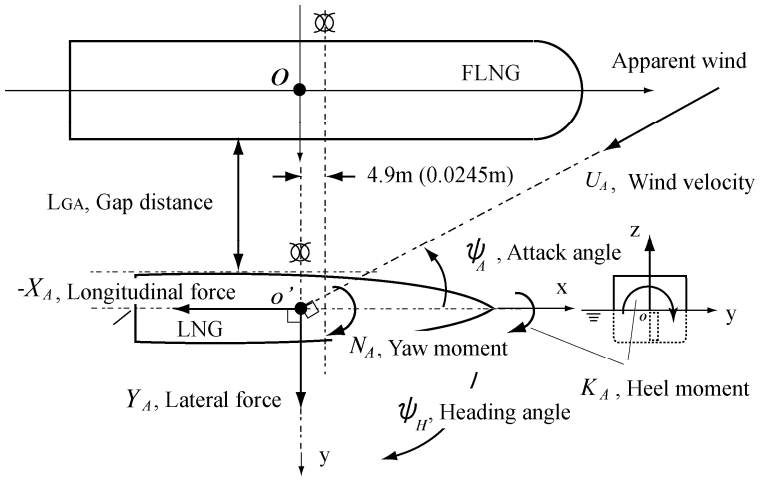

Figure 2. Coordinate system of wind force coefficients and basic positioning relation between FLNG and LNG.

2.3 Experimental setup:

Experimental setup in the wind tunnel is shown in Figure 3. Figure 4 is the experimental condition's photos in the wind tunnel. The wind tunnel experiments were carried out in our institute, NMRI. The tunnel is a Gottingen-type, breadth 3m × height 2m test section and has ability to make 30m/s wind velocity. The wind velocity selected for the investigations corresponds to a mean value of approximately 24m/s and Reynolds' number of 10^6 order for the model length, where the models are in turbulent flow condition, since the drag coefficients were independent of the Reynolds' number in this region. The wind velocity was arranged to be uniform in the vertical direction apart from the thin boundary layer over the wind tunnel floor. The boundary layer has a maximum thickness of approximately 10cm.

The LNG model was connected to the load cell in the turntable. Relative positions for two ships were changed by moving the FLNG model, where the gap distance on the relative position were set in 4.5m ~ 600m, the longitudinal relative position set in $\pm$80m, and the relative angle, that is heading angle in the Figure 2, set in $\pm$10deg in real ship scale respectively.

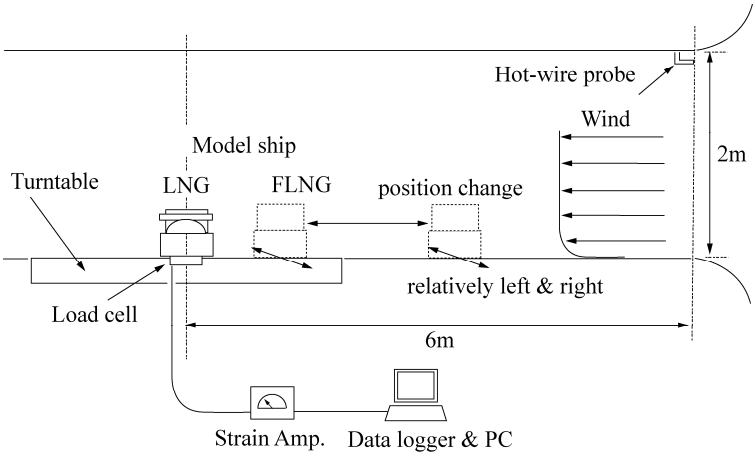

Figure 3. Experimental setup in the wind tunnel.

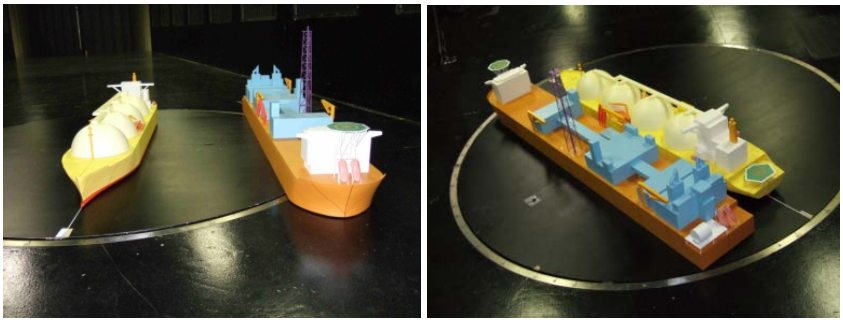

Figure 4. Photos of experimental conditions in the wind tunnel.

2.4 Sample of experimental results:

Figure 5 presents the four forces components of experimental results, longitudinal, lateral forces, C_X & C_Y, yaw, heel moments, C_N & C_K respectively. In the legend, the L_{GA} value that means for the gap distance as shown in Figure 2 has real ship order. The results of each condition were compared with the isolated LNG experimental results, which are the red line in the figures.

For C_Y & C_K in the $45<\psi_A<135$deg., as the LNG is in the shielding area of the FLNG, the experimental values of them are rapidly reduced getting closer to behind the FLNG. On the other hand, the C_N has the tendency of increase in the same area by contrast.

The shielding effect shown in the Figure 5 is expressed in the next chapter in considering the wind load estimation method on side by side offloading situation and approaching.

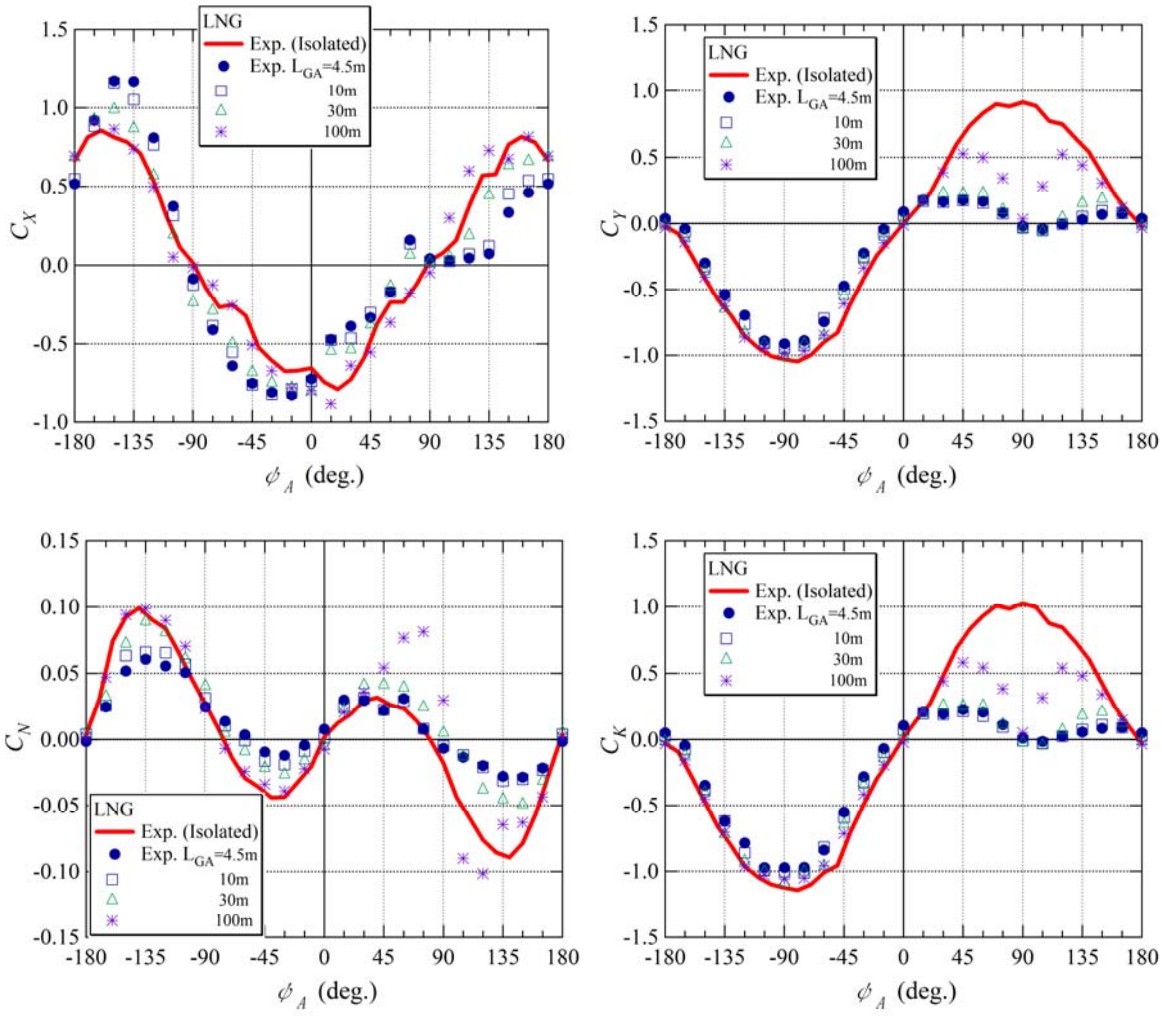

Figure 5. Example of experimental results on longitudinal, lateral forces, C_X & C_Y, and yaw, heel moments, C_N & C_K of LNG.

3 Wind load estimation method considered with shielding effect

One of the authors proposed the estimation method of wind force coefficients and moment coefficients indicated in Eq.1 for an isolated conventional ship, which has the best accuracy level rather than previous methods, using the physical components, namely the longitudinal-flow drag, cross-flow drag, lift and induced drags [5][6]. Although it is needless to say, estimation of wind load for a target ship results in obtaining to the wind force coefficients of that in general. To estimate wind force and moment coefficients, the 8 basic hull form parameters represented in Table 1, excluding the length between perpendiculars L_{PP}, the draught D, the depth d, are used in the estimation equations. The detail way to estimate the wind force coefficients is explained in next section. At this time, heel moment study is omitted, as the treat would be easily applied using the lateral force estimation method.

3.1 Estimation of wind force coefficients [5][6]:

The reference system origin is located at the intersection of the undisturbed free-surface and the amidship section of the ship according to Figure 2. And the 8 basic hull form parameters, illustrated in Figure 6, are used in the equations.

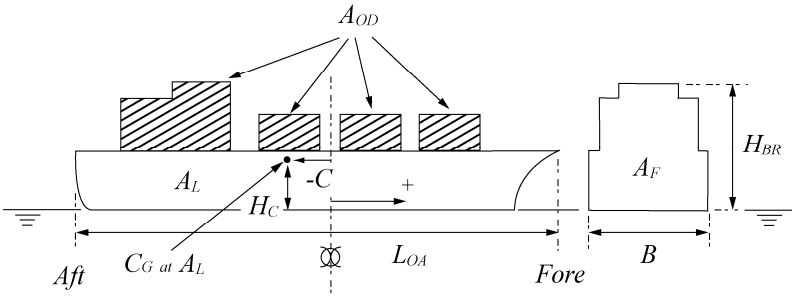

Figure 6. Definitions of each parameter on ship form in the wind force and moment estimations.

The longitudinal and lateral wind force coefficients C_X , C_Y are obtained using the following equations:

$$\begin{aligned} C_X(\psi_A) &= F_{LF}^{'} + F_{XLI}^{'} + F_{ALF}^{'} \\ &= C_{LF}\cos\psi_A \\ &+ C_{XLI}\left(\sin\psi_A - \frac{1}{2}\sin\psi_A\cos^2\psi_A\right)\cdot\sin\psi_A\cos\psi_A \\ &+ C_{ALF}\sin\psi_A\cos^3\psi_A \end{aligned} \tag{3}$$

$$\begin{aligned} C_Y(\psi_A) &= F_{CR}^{'} + F_{YLI}^{'} \\ &= C_{CR}\sin^2\psi_A \\ &+ C_{YLI}\left(\cos\psi_A + \frac{1}{2}\sin^2\psi_A\cos\psi_A\right)\cdot\sin\psi_A\cos\psi_A \end{aligned} \tag{4}$$

$F_{LF}^{'}, F_{XLI}^{'}, F_{ALF}^{'}$ mean the terms of longitudinal-flow drag, lift and induced drag, and additional longitudinal drag, respectively. And $F_{CF}^{'}, F_{YLI}^{'}$ are the cross-flow drag, and lift and induced drags in the lateral direction components. Each coefficient in Eq.3 and 4 is calculated from the following equations.

1) The cross-flow and longitudinal-flow coefficient C_{CF} & C_{LF} :

$$C_{CF} = \alpha_0 + \alpha_1\frac{A_F}{BH_{BR}} + \alpha_2\frac{H_{BR}}{L_{OA}} \tag{5}$$

$$\begin{aligned} C_{LF}^{0^\circ\le\psi\le90^\circ} &= \beta_{10} + \beta_{11}\frac{A_L}{L_{OA}B} + \beta_{12}\frac{C}{L_{OA}} \\ C_{LF}^{90^\circ\le\psi\le180^\circ} &= \beta_{20} + \beta_{21}\frac{B}{L_{OA}} + \beta_{22}\frac{H_C}{L_{OA}} + \beta_{23}\frac{A_{OD}}{L_{OA}^2} + \beta_{24}\frac{A_F}{B^2} \end{aligned} \tag{6}$$

2) The lift and induced drag coefficient C_{YLI} in the term of $F_{YLI}^{'}$:

$$C_{YLI} = \pi\frac{A_L}{L_{OA}^2} + C_{YM} \tag{7}$$

The first term in the Eq.7 stands for the liner lift component and the second is the corrective term affected from ship hull form above sea level. The coefficients C_{YM} separated in the wind direction are,

$$C_{YM}^{0^\circ \le \psi \le 90^\circ} = \gamma_{10} + \gamma_{11}\frac{A_F}{L_{OA}B}$$
$$C_{YM}^{90^\circ \le \psi \le 180^\circ} = \gamma_{20} + \gamma_{21}\frac{A_{OD}}{L_{OA}^2} \quad (8)$$

3) The lift and induced drag coefficient C_{XLI} in the term of $F_{XLI}^{'}$:

$$C_{XLI}^{0^\circ \le \psi \le 90^\circ} = \delta_{10} + \delta_{11}\frac{A_L}{L_{OA}H_{BR}} + \delta_{12}\frac{A_F}{BH_{BR}}$$
$$C_{XLI}^{90^\circ \le \psi \le 180^\circ} = \delta_{20} + \delta_{21}\frac{A_L}{L_{OA}H_{BR}} + \delta_{22}\frac{A_F}{A_L} + \delta_{23}\frac{B}{L_{OA}} + \delta_{24}\frac{A_F}{BH_{BR}} \quad (9)$$

4) The coefficient C_{ALF} in the term of $F_{ALF}^{'}$:

$$C_{ALF}^{0^\circ \le \psi \le 90^\circ} = \varepsilon_{10} + \varepsilon_{11}\frac{A_{OD}}{A_L} + \varepsilon_{12}\frac{B}{L_{OA}}$$
$$C_{ALF}^{90^\circ \le \psi \le 180^\circ} = \varepsilon_{20} + \varepsilon_{21}\frac{A_{OD}}{A_L} \quad (10)$$

The values of each coefficient are shown in Table 2.
The yaw moment coefficient is represented using the lateral wind force C_Y like these:

$$C_N(\psi_A) = C_Y(\psi_A)\cdot L_N(\psi_A)$$
$$= C_Y(\psi_A)\cdot\left[0.927\times\frac{C}{L_{OA}} - 0.149\times(\psi_A - \frac{\pi}{2})\right] \quad (11)$$

Table 2. Coefficients of non-dimensional parameter in the wind load estimating equations.

	i j : 0		1	2	3	4
α_j		0.404	0.368	0.902		
β_{ij}	1	-0.922	0.507	1.162		
	2	0.018	-5.091	10.367	-3.011	-0.341
γ_{ij}	1	0.116	3.345			
	2	0.446	2.192			
δ_{ij}	1	0.458	3.245	-2.313		
	2	-1.901	12.727	24.407	-40.310	-5.481
ε_{ij}	1	-0.585	-0.906	3.239		
	2	-0.314	-1.117			

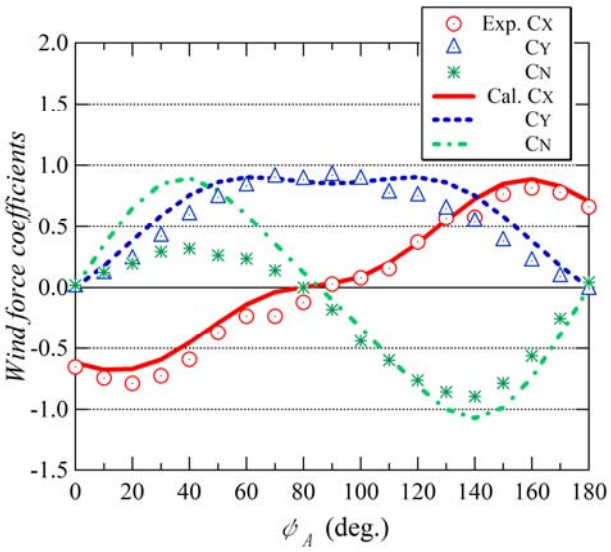

Figure 7. Comparison between the experimental results on wind force coefficients and calculated ones on isolated LNG.

Figure 7 shows as an example on calculated results comparing with the experimental ones for the LNG, shown in Table 1, in the isolated condition. The estimation method of wind force coefficients proposed by the author has enough accuracy to use in the ocean engineering situation, though in from ψ_A =0deg. to 90deg. has a little overestimation values.

Here, the wind load estimation method for a ship including shielding effect on the basis of the previous author's estimation method is explained in the next term. In this time, the study subject of the estimation method is limited as the case that the LNG is in the behind the FLNG under wind, that shows the right side in the each graph in Figure 5.

3.2 Basic concept of expression on wind shielding effect:

To consider the wind load estimation method with shielding effect, the following assumptions are taken into account for the ship wind load.

1) The wind shielding effect is disappeared at ψ_A =0 & 180deg. in the side by side situation for a FLNG and a LNG
2) The wind shielding effect has any value in proportion to the gap distance and the wind shielding area of two ships.

This second assumption was acquired from the wind tunnel experiments on a container ship with several kinds of forms on deck containers [7]. The gap distance is already defined as L_{GA} in Figure 2. Moreover, the shielding area length for wind direction is decided as L_{SA} shown in Figure 8. The points of reference getting L_{SA} are set at the each corner of a rectangular image form on FLNG outer frame, which the four black marks are placed in the figure. The LNG's fore and aft potion, drift angle against the FLNG influence on the L_{SA} value.

To investigate accuracy of the assumption of above mentioned second term, that is 2), the experimental results of the lateral force coefficient C_Y are taken up at first. Figure 9 shows the experimental results on reduced ratio of C_Y that is defined as $\Delta C_Y / C_Y$. For example, in case $L_{GA} / L_{OA} \approx 0.0$, where the LNG ship side approaches to the side of the FLNG infinite, the C_Y of the LNG becomes to have closely zero value (In this case, the reduced ratio $\Delta C_Y / C_Y$ becomes nearly equal to 1.0.) because of the true shielding position of the FLNG from wind.

In proportion to go the LNG outside, reducing shielding situation, $\Delta C_Y / C_Y$ becomes to be zero. In ψ_A =90deg. the shielding effect of the FLNG remains for large L_{GA} / L_{OA} rather than the other wind direction cases. This wind shielding effect in ψ_A =90deg. can be considered as maximum level of ship to ship interaction. It is assumed that the trend shielding effect of ψ_A =90deg. is represented using the Gaussian distribution form like following coefficient:

$$C_{S1}^{'} = \Delta C_Y / C_Y = \exp\left\{-\left(\frac{L_{GA}}{L_{OA}}\right)^2 / 2a_0^2\right\}, \qquad a_0 = 1.1 \tag{12}$$

The appropriation line of $\Delta C_Y / C_Y$ represented in Eq.12 depending on L_{GA} / L_{OA} is shown in Figure 9 as red dashed line. In the Eq.12 the experimental coefficient a_0 is decided as 1.1 from one ship's type experiments on the FLNG and the LNG. This coefficient is naturally affected by the external size and form of them. It is necessary to collect the information of the shielding effect for experimental results, rational theory and computational calculated study etc.

On the other hands, in case that the LNG is in near side of the FLNG (L_{GA} / L_{OA} =0.015~0.35), the ratio L_{SA} / L_{OA} becomes very important factor for $\Delta C_Y / C_Y$ without largely depending on the various wind directions as shown in Figure 10. The trend of the experiments is generally represented high-order function. In case of Figure 10's result, the effect of the reduction of $\Delta C_Y / C_Y$ is assumed to be multiplied the quartic function as follows:

$$C'_{S2} = \Delta C_Y / C_Y = (L_{SA} / L_{OA})^4 \tag{13}$$

From the results of Figure 9 and Figure 10, it becomes clear that the parameters of L_{GA} / L_{OA} and L_{SA} / L_{OA} have important role for wind load shielding effect. Then referencing on the relation Eq.12 and 13 each component of wind force coefficients is considered from next section.

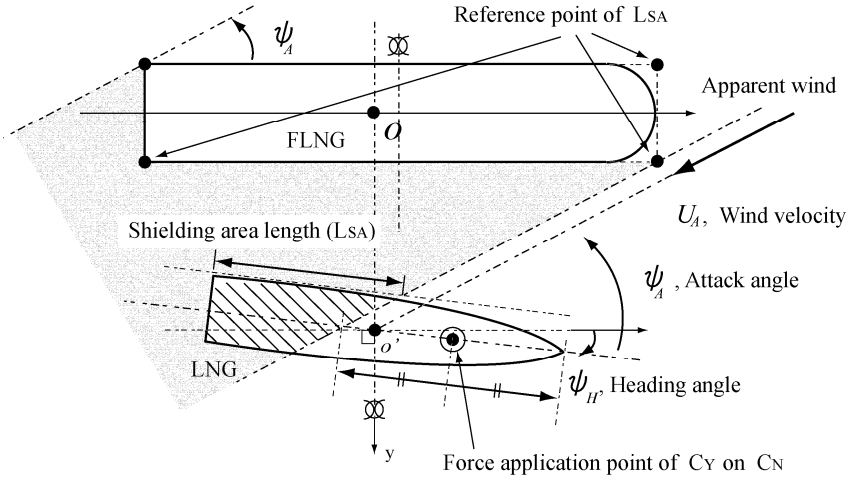

Figure 8. Definition of the shielding area length projected to LNG.

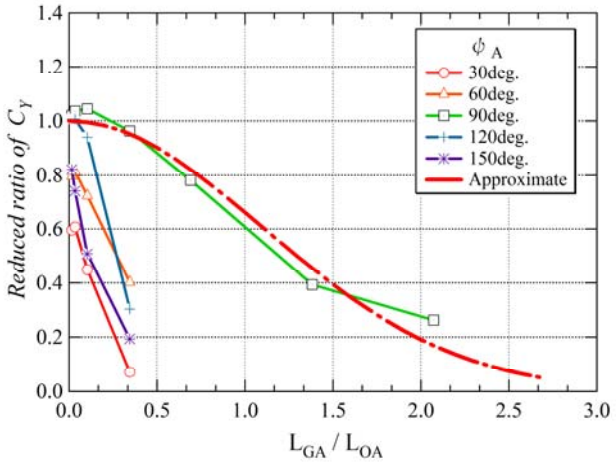

Figure 9. Experimental results of reduced ratio on C_Y and appropriation line of $\Delta C_Y / C_Y$ depending on L_{GA} / L_{OA}.

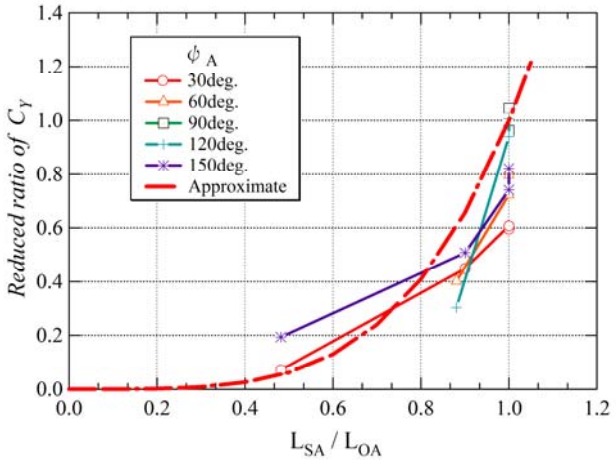

Figure 10. Experimental results of reduced ratio on C_Y and appropriation line of ΔC_Y / C_Y depending on L_{SA}/L_{OA} (L_{GA}/L_{OA} =0.015~0.350) .

3.3 Longitudinal force coefficient:

The longitudinal force coefficient, C_X , of the original method is consist of the longitudinal flow drag, lift & drag and additional force caused by the 3-dimentional flow effect as shown in Eq.3. It is also considered that each component in Eq.3 is affected by the wind shielding. Using the trend of the shielding effect obtained from Section 3.2, the effectiveness term on the effect is added in Eq.5.

$$\begin{aligned} C_X^{'}(\psi_A) &= (1-a_1 C_{S1} C_{S2})\left(F_{LF}^{'} + F_{XLI}^{'} + F_{ALF}^{'}\right) \\ C_{S1} &= \exp\left\{-\left(\frac{L_{GA}}{L_{OA}}\right)^2 / 2a_2^2\right\} \\ C_{S2} &= (L_{SA}/L_{OA}) \end{aligned} \tag{14}$$

Here, a_1 , a_2 are decided as 0.69 and 0.20 respectively to fit the experimental trend. The calculated results using Eq.14 are presented in Figure 11 with the experimental results. In order to make decision of a_2 value, it is referred that in case L_{GA} =100m the shielding effect is mostly vanished in the experimental data.

3.4 Lateral force coefficient:

The lateral wind force coefficients C_Y are defined using the cross-flow drag, and lift and induced drags in the original method. Authors modify the Eq.5 including the shielding effect as the same way of the C_X . As mentioned above, the lateral wind force has much relationship L_{GA}/L_{OA} and L_{SA}/L_{OA} ratio. Referencing the Figure 9 and 10, and using the original estimation of Eq.4, the equations of C_Y including the shielding effect are like the following:

$$\begin{aligned} C_Y^{'}(\psi_A) &= (1-C_{S3}C_{S4})\left(F_{CR}^{'} + F_{YLI}^{'}\right) \\ C_{S3} &= \exp\left\{-\left(\frac{L_{GA}}{L_{OA}}\right)^2 / 2b^2\right\}, \quad b = 1.1 \\ C_{S4} &= (L_{SA}/L_{OA})^4 \end{aligned} \tag{15}$$

Figure 12 shows the comparison between the experimental results on C_Y and calculated ones. The calculated results using Eq.15 is expressing the experimental results in general.

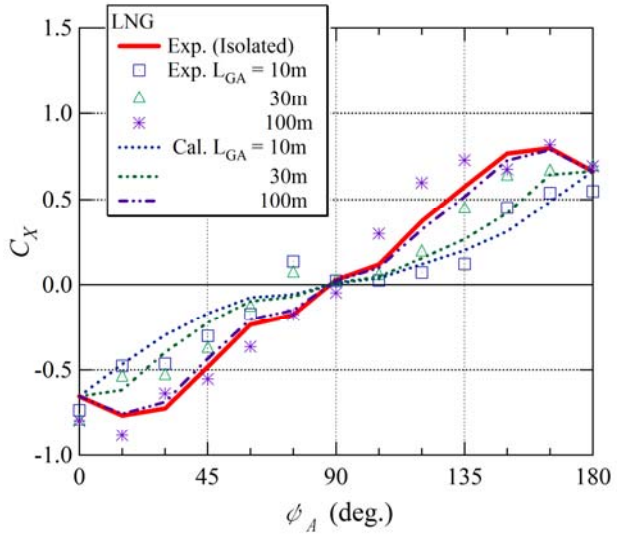

Figure 11. Comparison between the experimental results on C_X and calculated ones (Relative position of target ships is shown in Figure 2.).

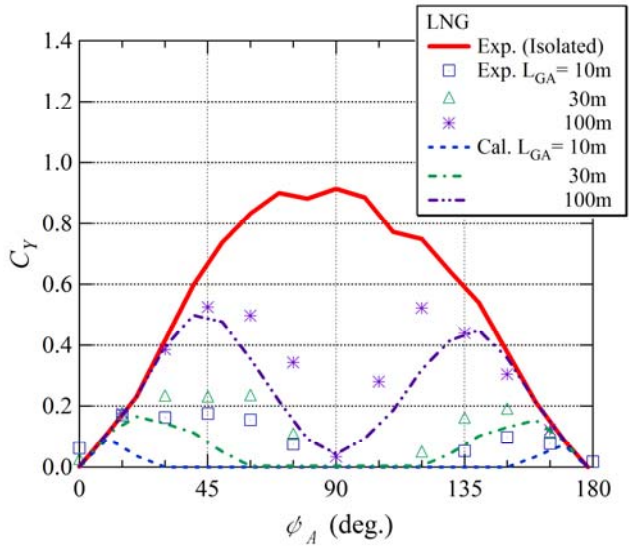

Figure 12. Comparison between the experimental results on C_Y and calculated ones (Relative position of target ships is shown in Figure 2.).

3.5 Yaw moment coefficient:

The yaw moment coefficients C_N in the original method is calculated using the lateral wind force C_Y and the non-dimensional moment levers L_N. The L_N are obtained from the experiments like Figure 13. In usual at the neighboring ψ_A=90deg., the levers L_N approaches to near zero. In shielding cases, however, as strong wind flows at the ship bow or stern area rather than at the mid-ship, the point of application of wind force keeps large value in the many wind direction.

To express the formulation on the C_N, the lateral force estimation method in Section 3.4 affected by shielding effect is used in the equation and the shielding effect to moment lever is also included in present version L_N. Considering the L_N formulation, following plans are picked out:

1) The force application point of yaw moment works on the center line for breadth and at the center of no shielding area for length direction as shown in Figure 8.
2) The trend of the L_N is much nonlinear in case of 90deg.$<\psi_A<$180deg. The results of small gap distance are ignored for

expressing the L_N formulation, since the C_N values of those ranges are very small rather than the other cases.

As final decision, non-dimensional moment lever L_N including shielding effect is expressed as follows:

$$\begin{aligned} L_N^{'}(\psi_A) &= L_{N0}(\psi_A)\cdot(1-C_{S3}) + L_{NS}(\psi_A)\cdot C_{S3} \\ L_{NS}(\psi_A) &= \pm 0.25\, C_{S5} \quad (\frac{L_{SA}}{L_{OA}} < 0.5) \\ &= \pm C_{S5}\frac{L_{SA}}{2L_{OA}} \quad (0.5 \le \frac{L_{SA}}{L_{OA}}) \quad \begin{Bmatrix} 0 \le \psi_A \le \pi/2 \\ \pi/2 < \psi_A \le \pi \end{Bmatrix} \end{aligned} \qquad \text{in } \frac{L_{SA}}{L_{OA}} \neq 0 \tag{16}$$

where,

$$C_{S5} = \begin{cases} 0.44\ (0 \le \psi_A \le \pi/2) \\ 0.63\ (\pi/2 < \psi_A \le \pi) \end{cases} \tag{17}$$

The L_{N0} is the moment lever L_N in Eq.11.

As a final form, the yaw moment coefficient with wind shielding effect is represented as follows:

$$C_N^{'}(\psi_A) = C_Y^{'}(\psi_A)\cdot L_N^{'}(\psi_A) \tag{18}$$

Figure 13 shows the comparison between the experimental results on L_N and calculated ones. And Figure 14 also shows the comparing results of C_N. In case of L_{GA}=100m, C_N has unique value having larger than them of the other cases. The formulation Eq.16 with Eq.15 has good agreement for estimating the C_N in shielding condition.

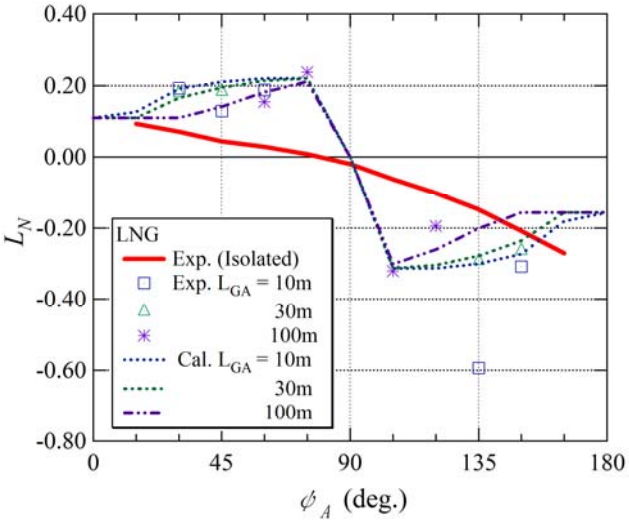

Figure 13. The non-dimensional moment levers L_N comparing experimental results and calculated ones (Relative position of target ships is shown in Figure 2.).

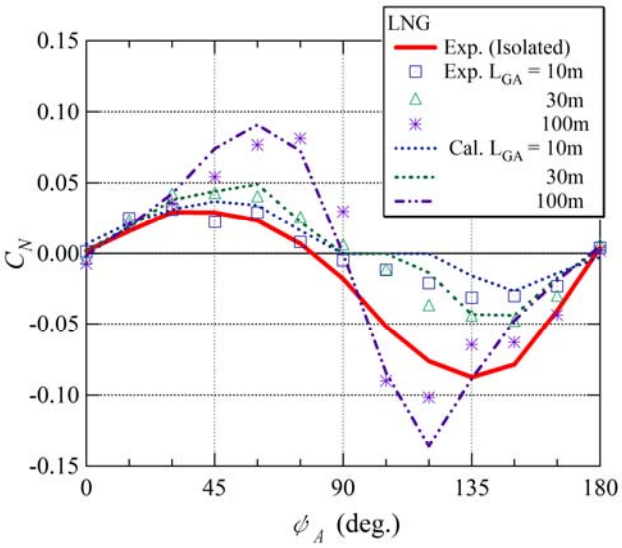

Figure 14. Comparison between the experimental results on C_N and calculated ones (Relative position of target ships is shown in Figure 2.).

4 Operational assessment on ship manoeuvring under strong wind using wind force estimation method with shielding effect for a LNG ship

In order to confirm the wind shielding effect, ship manoeuvring simulation for the LNG is applied to side by side situation along with the FLNG. The 3DOF MMG method is used in the simulation like as ordinal way [8~10]. The equations are defined as follows:

$$\begin{aligned}(m+m_x)\dot{u}-(m+m_y)vr &= X_{H0}+X_P+X_R+X_A\\ (m+m_y)\dot{v}+(m+m_x)ur &= Y_H+Y_R+Y_A\\ (I_{ZZ}+J_{ZZ})\dot{r} &= N_H+N_R+N_A\end{aligned} \tag{19}$$

The ship mass and added mass and the yaw moment of inertia of the ship are denoted by m , I_{ZZ} etc. whereas the longitudinal, lateral and yaw velocities with respect to the centre of gravity of the ship are designated u , v and r . Furthermore, the external forces and moments designated X , Y , N have components arising from the hydrodynamic characteristics of the hull, the propeller generated thrust, the rudder and the wind forces acting on the hull using the suffixions H , P , R , A . In that case, X_{H0} means calm water resistance going straight forward, and Y_H , N_H are used the experimental data for similar ship's type in the reference [11].

Figure 15 shows the LNG drifting motion based on the simulation. The ship approaches near zero speed. Then, the suffixions P , R terms have limited small values. Mainly Eq.19 is equivarium by Y_H , N_H and wind force terms. The upper figure is the result of no FLNG situation in U_A=30m/s, ψ_A=135deg., and the lower one is the side by side situation with FLNG in same condition. Moreover, Figure 16 shows the LNG heading angle in same strong wind. Although the calculated weather situation is very severe and tough for the ship manoeuvring and in the rare case, the LNG heading angle shown in Figure 16 has large difference in the reason of different ship situation.

Figure 17 shows the example of the maximum heading angle of the LNG, as the absolute value, under the weather condition of U_A=30m/s, ψ_A=90deg. The vertical and horizontal axes are described as based on the FLNG position. At first, the LNG is placed various downwind positions against the FLNG. In drifting situation by the manoeuvring simulation, maximum heading angle of the ship in the 3 minutes is picked up. The case that the aft section of the LNG is exposed to strong wind makes large heading angle in closed position for the FLNG.

For the view points of safety operation on side by side, the exact manoeuvring simulation including the shielding effect will be made into necessity in future.

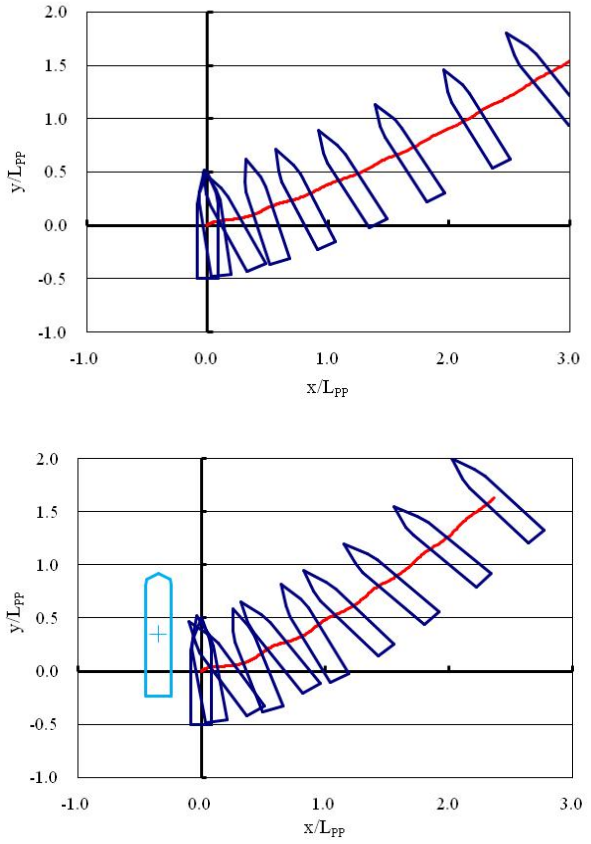

Figure 15. LNG drifting motion based on the ship manoeuvrability simulation under strong wind (U_A=30m/s, ψ_A =135deg., Upper; No FLNG situation, Lower; Side by side situation with FLNG).

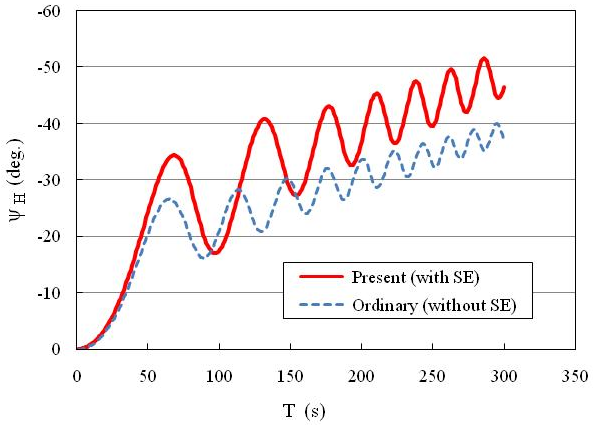

Figure 16. LNG heading angle under strong wind (U_A=30m/s, ψ_A =135deg.).

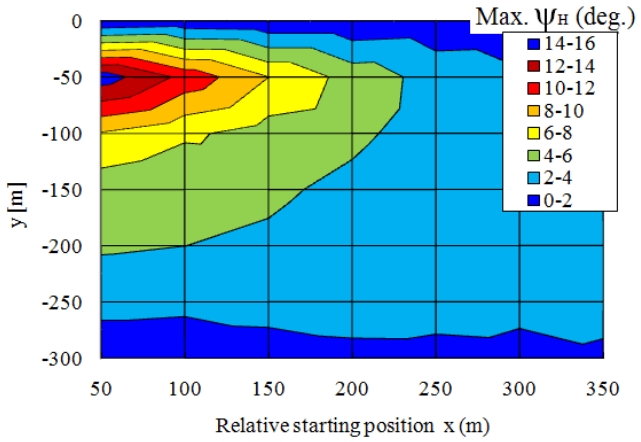

Figure 17. Maximum LNG heading angle under strong wind (U_A=30m/s, ψ_A =90deg.).

5 Conclusions

Assuming the increasing opportunity of the side by side offloading operation for FLNG and LNG carrier ships, the way of estimate the wind load in that situation is proposed in this paper. This trial is one of the examples since the used ship type is one case, but the way of thinking will be able to use the actual case of the operation. The results of this paper are summarized as follows:

1. Aerodynamic characteristics for the longitudinal, lateral wind forces and the yaw, heel moments of the shielding effect is investigated using the wind tunnel experimental results and the formulation of the estimation of wind load with the effect in case of side by side operation is proposed.
2. The shielding effect is mainly calculated by the geometrical position, and concept of the shielding area definition defined by the 4 corners of the ship form.
3. The non-dimensional parameters of the L_{GA}/L_{OA} and the L_{SA}/L_{OA} become important factor for representing the shielding effect of a ship.
4. The effect of the estimated result is shown with simulation on the mathematical modeling of a LNG ship. It is shown that the present method of estimating wind load has important role to calculate the ship manoeuvring motion in the operational stage of the side by side operation.

References

[1] Tannuri A, E, Fucatu H, C, et al., “Wind Shielding Effects on DP System of a Shuttle Tanker”, Proceedings of the 29th International Conference on Ocean, Offshore and Arctic Engineering (OMAE2010), OMAE2010-20148, China, 2010.
[2] Voogt A, “Effect of Heading Control on LNG Offloading”, Proceedings of the Nineteenth International Offshore and Polar Engineering Conference (ISOPE2009), pp.199-204, Osaka, 2009.
[3] Voogt A and Brugts H, “Numerical Simulations to Optimize Offshore Offloading Operations”, Proceedings of 2010 Offshore Technology Conference (OTC2010), OTC20638, 2010.
[4] Bruin, A, C, “Initial development of a method to account for wind shielding effects on a shuttle tanker during FPSO offloading”, National Aerospace Laboratory NLR, NLR-CR-2003-018, Germany, 2003.
[5] Fujiwara, T, Ueno, M, and Ikeda, Y, “A New Estimation Method of Wind Forces and Moments acting on Ships on the basis of Physical Component Models”, J the Japan Society of Naval Architects and Ocean Engineers, Vol.2, pp.243-255, 2005. (in Japanese)
[6] Fujiwara, T, Ueno, M, and Ikeda, Y, “Cruising Performance of a Large Passenger Ship in Heavy Sea”, Proceedings of the Sixteenth International Offshore and Polar Engineering Conference (ISOPE2006), pp.304-311, 2006.
[7] Fujiwara, T, Tsukada, Y, Kitamura, F, Sawada, H and Ohmatsu, S, “Experimental Investigation and Estimation on Wind Forces for a Container Ship”, Proceedings of the Nineteenth International Offshore and Polar Engineering Conference (ISOPE2009), pp.555-562, 2009.
[8] Fujiwara, T, Ueno, M, and Ikeda, Y, “Cruising Performance of Ships with Large Superstructures in Heavy Sea - 1st report: Added Resistance induced by Wind -”, J the Japan Society of Naval Architects and Ocean Engineers Vol.2, pp.257-269, 2005. (in Japanese)
[9] Tanaka, A, Yamagami, Y, Yamashita, Y and Misumi, E, “The Ship Manoeuvrability in Strong Wind”, J the Kansai Society of Naval Architects, Vol.176, pp.1-10, 1980. (in Japanese)
[10] Kijima K, Katsuno T, Nakiri Y et al., “On the Manoeuvring Performance of a Ship with the Parameter of Loading Condition”, J the Society of Naval Architects of Japan, Vol.168, pp.141-148, 1990.
[11] Obokata, J, Sasaki, N and Nagashima, J, “On the Estimation of Current Force induced on a Ship Hull by Some Model Tests”, J the Kansai Society of Naval Architects, Vol.180, pp.47-57, 1981. (in Japanese)